J. Membrane Biol. 61, 39–54

The Journal of
Membrane Biology

Radio-Frequency Bioeffects at the Membrane Level: Separation of Thermal and Athermal Contributions in the Characeae

William F. Pickard and Yousri H. Barsoum

Department of Electrical Engineering, Washington University, Saint Louis, Missouri 63130

Summary. Single cells of *Chara braunii* and *Nitella flexilis* were placed in a microstrip exposure apparatus and subjected to isolated bursts of radio-frequency irradiation. Their electrical responses were observed both extra- and intracellularly and found to be in accordance with theoretical predictions. In particular, the cell membrane displays rectifier-like behavior up to a cutoff near 10 MHz; this cutoff implies for the principal current carriers a transit time through the membrane of roughly 50 nsec and a mobility within the membrane approximately one-fifth that of potassium in free solution. An electrical response of purely thermal origin was also detected; it was separated from the athermal rectifier response on the basis of rise time and frequency dependence. This is believed to be the first instance in which (i) a biological effect of radio-frequency radiation has had its thermal and athermal components clearly separated and (ii) a primary effect of ion transit time through the membrane has been directly detected.

Key words: Characeae, electrogensis, ion flux, radio-frequency bioeffects, rectification, transit time.

In studies of the interaction of radio-frequency and microwave radiation with living systems, a question always asked of any observed effect is whether it is "thermal" or "athermal"[1]. And as often as not, the answer given becomes controversial because (*cf.* Stuchly, 1979) the criteria for this dichotomization were not clearly delineated, or seemed to have been capriciously chosen, or were subjectively applied. That this actually might be a problem may at first seem surprising given that the extremes of thermal phenomena (e.g., microwave cooking) and athermal phenomena (e.g., resonance absorption by a molecule) are so obviously different. But there is a large grey area between. And, in any given instance, the distinction should ultimately be based not upon the absence of patently catastrophic heating but upon the congruence of the observed phenomena with the explicit predictions of a concrete model; and the designation "athermal" should be reserved for phenomena characterized by the presence of modes of behavior which would be unlikely to arise if the effect were based solely upon an increase in the random kinetic motion of the system's constituent molecules.

More precisely, a given radio-frequency bioeffect should be characterized as "athermal" only after:

1) The anticipated behavior due to classically predictable RF heating has been deduced and shown to be contrary to experimental fact.

2) A model which does not depend upon increased thermal agitation for its operation has been formulated and shown to be in accordance with experimental fact.

If experimental fact is well explained by a model based upon classical RF heating, the effect should be called "thermal"; if the data suffice for neither label, the effect should be called "equivocal".

Various possible candidates for athermal mechanisms have been reviewed by, e.g., Bawin, Sheppard, and Adey (1978) and by Stuchly (1979). Specific mechanisms for athermal interaction at the level of the cell membrane have been set forth by, e.g., Spiegel and Joines (1973), Wachtel, Seaman, and Joines (1975), Barnes and Hu (1977), Pickard and Rosenbaum (1978), Offner (1979), and Cain (1980). And in the radio-frequency region (say 0.1–50.0 MHz) the most fully worked out membrane mechanism is that of direct rectification of the applied field by the charge transporting systems of the membrane (Barnes & Hu, 1977; Pickard & Rosenbaum, 1978).

[1] The terms "athermal" and "nonthermal" are used interchangeably in the literature.

0022-2631/81/0061-0039 $03.20

Not only is direct rectification the best worked out athermal mechanism in the radio-frequency region, it is only at radio-frequencies and below that it is expected to be significant. This is because (Pickard & Rosenbaum, 1978) the transit times through the membrane of the charge carriers are expected to be of the order of 5 nsec or greater so that high frequency applied fields produce progressively less rectification, their influence becoming primarily that of gently dithering the charge carriers; i.e., at sufficiently high frequencies, the applied electric field will alternate in direction so quickly as to have little net effect on the motion of a carrier. Unfortunately, despite these interesting properties, direct radio-frequency rectification must be termed speculative since there has been little or no convincing evidence for either the existence of the behavior of the mechanism. The goal of this paper is to provide such evidence.

Theory

Expected Voltage Variation of the Effect

Placing a cell in an RF field results in the setting up of RF voltage gradients across its plasma membrane. These gradients should, in turn, modify current flow across that membrane. If then the current *vs.* voltage relation of the membrane is nonlinear (i.e., rectifying), this should change the charge on the membrane capacitance and shift the cell's resting potential. The theory of this shift in the steady-state limit (i.e., transit time very much less than RF period) has been given by Barnes and Hu (1977) and by Pickard and Rosenbaum (1978). It predicts that the resting potential offset $\Delta V[V]$ will be given by

$$\Delta V = \alpha_2 v_o^2 + \alpha_4 v_o^4 + \ldots \tag{1}$$

where the α's are constants, $v_o[V]$ comes from the voltage difference $\sqrt{2}\, v_o \cos \omega t$ applied to the membranes, and the applied frequency f [Hz] is given by $f = \omega/2\pi$. The prediction of the α's requires a knowledge of the current-voltage characteristics of the membrane which is considerably more detailed than usually available.

It should be noted that the detection of a resting potential shift which is quadratic in v_o is but equivocal evidence for the rectification mechanism, since the thermal input to the system will also be quadratic in the applied field and therefore in v_o (*cf.* Appendix I).

Applied Fields

Suppose a long cylindrical cell is oriented with its axis perpendicular to an electric field of the form $\vec{E} = \hat{x}\sqrt{2} E_{\text{rms}} \cos \omega t$. Let the cell's plasma membrane be characterized by a conductance per unit area $G[\text{S/m}^2]$, a capacitance per unit area $C[\text{F/m}^2]$, and an admittance per unit area $Y = G + j\omega C$. Let complex conductivity of the cell's exterior be $\zeta_e = \sigma_e + j\omega\varepsilon_e$ where $\sigma_e[\text{S/m}]$ is the conductivity of the bathing medium and $\varepsilon_e[\text{F/m}]$ its permittivity; similarly, for the cell's interior, let the complex conductivity be $\zeta_i = \sigma_i + j\omega\varepsilon_i$. Then, if the cell radius is a[m], it can readily be shown (*cf.* Appendix I) that the resultant membrane voltage is

$$v(\theta, \omega; t) \doteq [2\sqrt{2}\, E_{\text{rms}} \cos\theta]\, \mathcal{RE}\left\{\frac{\zeta_e}{j\omega C}\, e^{j\omega t}\right\} \tag{2}$$

where θ [rad] is an angle measured from the x-axis and the notation $\mathcal{RE}$ means "the real part of." Below 5 MHz (*cf.* Appendix I) $|v| \propto 1/\omega$; but near 50 MHz, ζ_e has become capacitive and $|v|$ is roughly constant in ω.

If only the second order term of Eq. (1) is significant, then the technique of Pickard and Rosenbaum (1978) yields an effective value for v_o^2 of

$$[v_o^2]_{\text{eff}} = 2E_{\text{rms}}^2 \left|\frac{\zeta_e}{\omega C}\right|^2. \tag{3}$$

Hence, below 10 MHz the resting potential offset should vary roughly as the mean square applied field and inversely as the square of the frequency of that field.

Transit Time Effects

When the period of oscillation of the applied field ceases to be large compared to the average time it takes a charge carrier to move between a device's electrodes (here the cytoplasm and bathing medium of a cell), then the behavior of the device can change radically. Such effects, called transit time effects, are well known in electronics (*cf.* Dascălu, 1974) and are generally assumed to become important at and above frequencies given roughly by (Cooke, 1971)

$$\omega \hat{T} = 1 \tag{4}$$

wher $\hat{T}$[sec] is the time it takes the carrier to pass between the electrodes at zero perturbing field ($v_o = 0$). A crude theory of these effects on the cellular level (Appendix II) yields

$$\Delta V = \alpha_2 v_o^2 F(\omega \hat{T}) \tag{5}$$

where $F(\omega\hat{T}) \doteq 1$ for $\omega\hat{T} < 1$, then falls steadily to a zero at $\omega\hat{T} \approx \pi$, and exhibits a complicated (but low amplitude) comb structure for $\omega\hat{T} \gtrsim \pi$.

Time Constants

In their discussion of rectification, Pickard and Rosenbaum (1978) pointed out that, since both the heating of the fluid bathing a cell and the rectification itself should vary as E_{rms}^2, an experimental finding of quadratic E_{rms}-dependence for ΔV was evidence only for the existence of a bioeffect and not for the etiology of the bioeffect. But they also pointed out that if brief rectangular pulses of irradiation were employed then a direct rectification effect would yield an offset which rose with the electrical time constant of the cell's limiting membranes, whereas a thermal effect should rise with the thermal time constant of some critical portion of the exposure apparatus.

The time constant for charging by a rectifier should be very roughly

$$\tau_r = C/G \tag{6}$$

where τ_r is measured in seconds. For characean cells, measurements in this laboratory and also those commonly found in the literature (*cf.* Hope & Walker, 1975) yield $0.01 \lesssim C \leqq 0.02$ and $0.1 \lesssim G \lesssim 10$. Hence $0.001 \lesssim \tau_r \lesssim 0.2$. A typical value might be 10 msec.

If, as in the experiment to be described below, the heart of the exposure apparatus is a long rectangular channel filled with flowing bathing solution, then (*cf.* Carslaw & Jaeger, 1959) a crude measure of the principal time constant of the apparatus is

$$\tau_a = \frac{1}{\kappa \pi^2} \frac{w^2 h^2}{w^2 + h^2} \tag{7}$$

where τ_a is measured in seconds, where the channel is of width w[m] and height h[m], and where $\kappa (\doteq 0.14 \times 10^{-6}\ \text{m}^2/\text{sec})$ is the thermal diffusivity of the bathing solution. For a channel of the order of 1 $\times$ 2 mm, this yields $\tau_a \approx 1/2$ sec.

Thus, there is at least an order of magnitude gap between τ_r and τ_a, and it should be readily possible to distinguish rectification effects from heating effects if pulsed irradiation is used.

Materials and Methods

General Experimental Configuration

The overall electronic structure of the experiment is shown in Fig. 1, and specifics of the irradiation setup are shown in Fig. 2. The equipment was housed in a radio-frequency shielded room, and the preparation and first two stages of amplification were enclosed in a Faraday cage within that room.

The basic fluidic configuration was a modification of that of Roa and Pickard (1976). Bathing solution, from a reservoir about 1 m above the irradiation region, was conducted to the influx tube by way of a needle valve and a flowmeter. It then passed through a polyethylene tube imbedded in a thermoelectric cooling module (Pickard, 1973) and emerged to enter the channel. From the channel it flowed under gravity to a surge tank and then down a wick-filled rubber tube to a waste reservoir on the floor. By adjusting the needle valve and the emergence of the wick (not shown in Fig. 2) into the surge tank, a smooth flow of temperature-controlled liquid was maintained at roughly 1 ml/min. Dropwise flow must be avoided since drop formation is a potent source of electrical noise. The long runs of fluid in insulating tubes serve as 60 Hz antennas and make mandatory the dual grounding of the solution shown in Fig. 2; the silver ground plane alone did not prove adequate to eliminate completely the 60 Hz induced currents along the channel.

In an experiment, a cell was placed in the channel with its upstream end under the center conductor and was either (i) impaled by the signal pipette some 2 to 4 mm downstream from the center conductor (intracellular recording) or (ii) had the shank of the pipette lightly pressed against it to hold it steady in the channel (extracellular recording). The reference pipette was placed several mm upstream from the center conductor, normally symmetrical with the signal pipette. Recordings were taken differentially from the two pipettes to reduce 60 Hz interference.

Rectangular pulses of RF irradiation were given (in synchrony with the 60 Hz line power) once every 6.3 sec; this spacing was chosen to be long compared to the anticipated electrical time constants of the cell and also to give the several electronic filters (*cf.* Fig. 1*B*) time to relax back to their steady states. Pulses were typically 250 msec in duration since this was several times greater than both the anticipated electrical time constants of the cells and also the rise times observed for the putatively nonthermal effects studied; pulse length was, however, variable from roughly 10 μsec to over 10 sec.

The bandwidth ultimately selected (0.13–1600 Hz) was a compromise between a desire to maintain signal fidelity and a desire to reduce noise. The low frequency 3-dB point was chosen to cut out some of the worst low frequency excess noise (Roa & Pickard, 1976) but carried with it the penalty of introducing an exponential droop (time constant $\sim$1 sec) into rectangular steps. The high frequency 3-dB point was chosen in accordance with the Elmore relation (*cf.* Lindquist, 1977) to make the system's rise time ($\sim$0.2 sec) short compared to any responses expected from the preparation; but it was kept low to reduce high frequency white noise and to squelch any residual RF which might produce saturation or other nonlinear behavior in the ac-coupled amplifier.

The signal to noise ratio of a noisy signal will be improved roughly $\sqrt{N}$-fold if N phase-locked repetitions of the signal are added together. The signal averager was normally triggered about 40 msec before the start of an irradiation pulse, following which it digitized the incoming analog signal at 2048 time points spread across the pulse, added the values so obtained to those stored in memory, and displayed a running total. If several challenges are to be delivered to the same cell, there is a practical upper limit of about 30 min per experiment; this correspond to $N \approx 300$ or a 17-fold enhancement. If detailed frequency spectra are desired, the time constraints are somewhat more stringent: for these studies N was set equal to 20, and this seemed to provide adequate enhancement of the signal in a reasonable amount of time.

The square wave generator was used to inject square pulses of current through the signal pipette and across the cell membranes for the purpose of determining G and C. The voltage offsets so produced had their dc levels removed in the scaling amplifier and the resistive contribution of the signal pipette cancelled leaving a series of pulses with height proportional to G and time constant C/G.

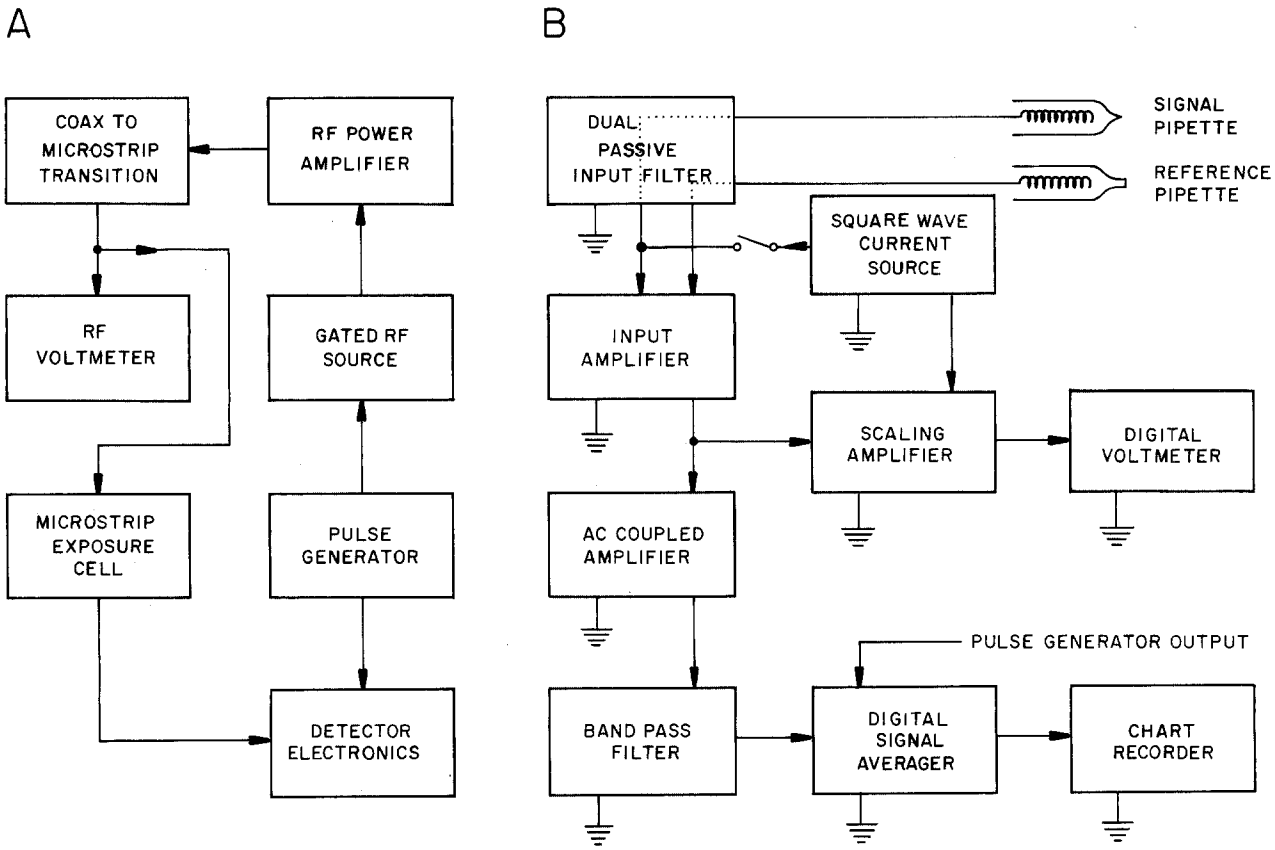

Fig. 1. Radio-frequency irradiation circuitry. (*A*): Overall block diagram. (*B*): Detailed block diagram of the detector electronics. The digital signal averager was a TN-1505 (Tracor Northern, Middleton, WI 53562). The input amplifier was the ultra-low noise PAR model 113 (Princeton Applied Research Corporation, Princeton, NJ 08540) set to a dc-300 kHz pass band (6 dB/octave rolloff) and a gain of 20×; its input impedance was 100 MΩ shunted by 15 pF. Electrical characteristics of the other key components were as follows. Input filter: dc-2800 Hz (6 dB/octave); gain 1×. Scaling amplifier: gain $\frac{1}{2}\times$ (inverting). Ac coupled amplifier: 0.13–1600 Hz (6 dB/octave); gain 500× (inverting). Band pass filter: 0.025–2500 Hz (24 dB/octave); gain 1×. The scaling amplifier also contained circuitry which could be used for single pipette measurements of *G* and *C*

Pipettes

Agar-KCl micropipettes were made by the technique of Pickard and Roa (1976). They were coupled to the lead wires of the detector by short lengths of silver wire electrolytically coated with silver chloride.

The signal pipettes possessed external tip diameters of the order of 5 μm and had, when immersed in the fluid-filled channel, impedances to ground of roughly 600 kΩ. The external reference pipettes had tip diameters of perhaps 15 μm.

Exposure Cell

The cell used for exposing the test specimens (Fig. 2) was a sandwich consisting of a silver foil ground sheet, a polyacrylate sheet into which the channel was cut, and a narrow silver foil strip running perpendicular to the channel. This microstrip structure was then fastened to the copper ground plate with cyanoacrylate adhesive and tack soldered at an edge point for electrical contact. To reduce electrical interference associated with control of the thermoelectric cooling module, the copper plate was separated from the module by a sheet of sintered Al_2O_3 (porcelain) of high thermal but negligible electrical conductivity.

Early models of the exposure cell in which the basic construction of the channel region involved a variety of metals subsequently gold plated (in an attempt to produce a physiologically neutral surface) invariably developed cracks, discolorations, and zones of inhomogeneous electrical activity; the net results were (i) longitudinal dc currents which could shift the dc level of the channel by several mV per cm and (ii) surface deposits which themselves produced a low level rectification of the RF. The all-silver model was free of these electrophysical artifacts provided (i) that the silver surfaces of the channel were polished with cellulose tissue and left scrupulously clean between uses, (ii) that they were lightly rubbed with crocus cloth about twice a week, and (iii) that cell cytoplasm was not allowed to deposit on them. No adverse biological effects attributable to silver were ever detected: the cells used normally maintained their resting potentials and streamed vigorously for at least two hours after impalement.

Electric fields between the strip and the ground plane should be transverse electromagnetic mode up to a frequency of (*cf.* Mittra & Itoh, 1974)

$$f_{H1} \doteq \frac{c}{4d(\varepsilon_r - 1)^{\frac{1}{2}}} \tag{8}$$

where $c[=2.997\ldots\times 10^8$ m/sec] is the velocity of light in vacuum, and where d[m] is the thickness of the dielectric slab and ε_r [dimensionless] its relative permittivity. For the polyacrylate ($\varepsilon_r \doteq 2.7$) slab ($d \doteq 1.6$ mm) used here, $f_{H1} \doteq 35$ GHz. This is well above the frequency range studied. TEM-mode fringing fields are

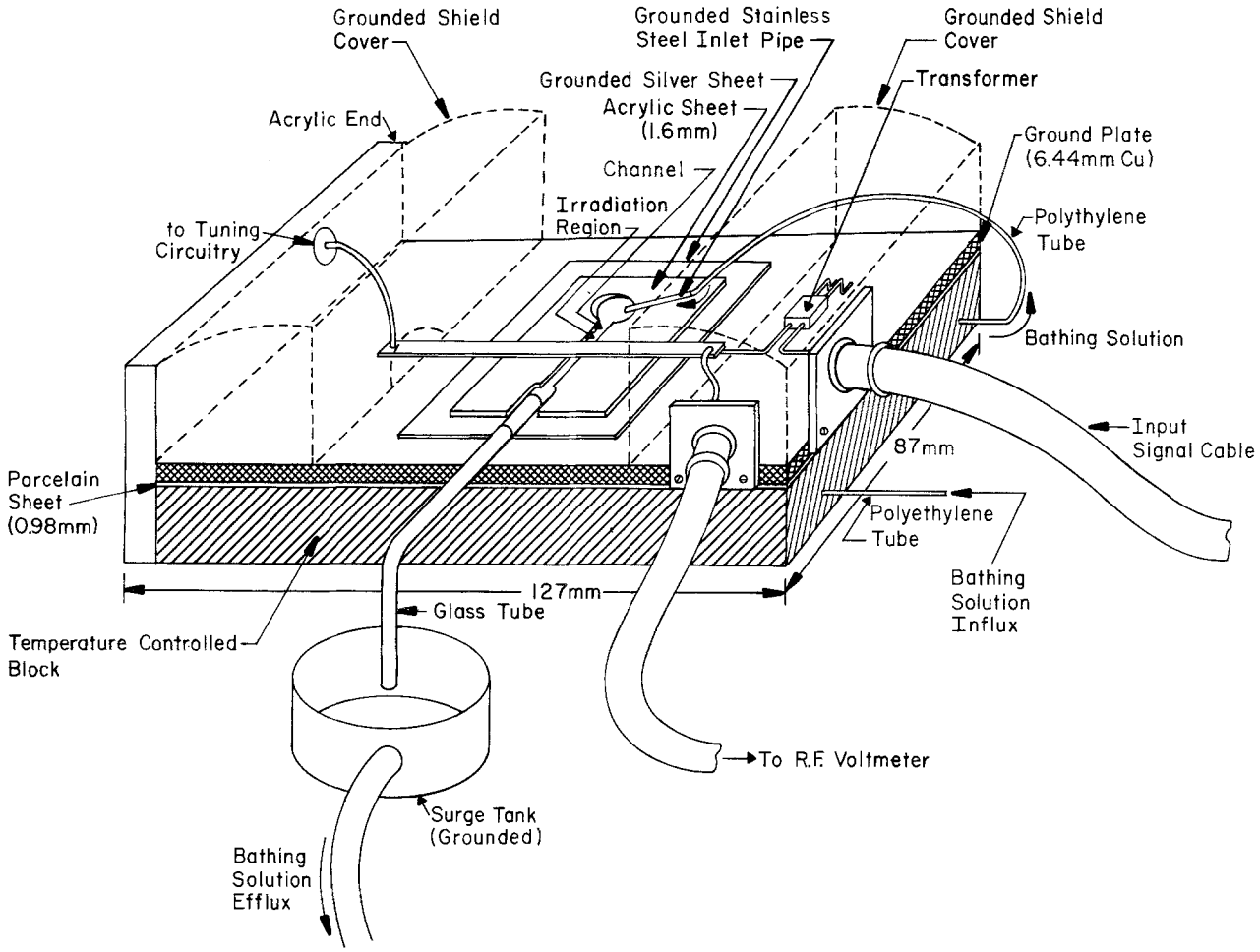

Fig. 2. Details of irradiation setup. Not shown are a cell placed under and downstream from the center conductor, a signal pipette placed downstream from the center conductor, and a reference pipette placed upstream from the center conductor. The dimensions of the irradiation region are: center conductor width, 2.4 mm; channel width, 1.0 mm; channel depth, 1.6 mm. The pipettes were connected to the input filter and the input amplifier by a light-weight tinsel cord to reduce input loop area and magnetic pickup of 60 Hz

well known to fall off very rapidly near the edge of the strip, and measurements at 250 kHz made using the signal pipette indicate that a relative pickup of 1.00 at the strip edge is reduced to 0.55 at 1 mm, 0.23 at 2 mm, 0.066 at 3 mm and 0.014 at 4 mm.

The practical high frequency limit of the exposure cell and its associated circuitry is that it behave like a lumped impedance at the wavelengths used. That is,

$$f_{H2} \doteq \frac{c}{10L\sqrt{\varepsilon_r}} < f_{H1} \tag{9}$$

where L[m] is a characteristic maximum dimension of the exposure cell and its associated components. Since $L < 50$ mm, $f_{H2} \doteq 300$ MHz.

Solutions

The solutions used were all based upon the electrogenic artificial pond water (EAPW) developed by Pickard (1973): 2.5 mM KCl, 2.5 mM NaCl, 0.5 mM $CaCl_2$, 0.5 mM $MgCl_2$, 0.5 mM N-2-hydroxyethylpiperazine-N-2-ethanesulfonic acid (HEPES), 0.25 mM NaOH; its pH at room temperature is approximately 7.35. It has been shown (Pickard, 1973) that a characean cell bathed by this solution should exhibit a vacuolar resting potential no more negative than -100 mV unless active charge transport is occurring.

Biological Materials

Chara braunii Gm. was collected locally and maintained in large tanks in the laboratory. *Nitella flexilis* (L.) Ag., purchased from the Connecticut Valley Biological Supply Co. (Southampton, MA 01073), was similarly maintained.

On the evening before an experiment robust appearing, vigorously streaming, epiphyte- and incrustation-free cells approximately 6 mm long were trimmed from their thalli and allowed to equilibrate overnight in EAPW. The length constraint resulted in young internodal cells and penultimate branchlet segments predominating heavily.

Following impalement, the signal pipette was retracted slightly so that the cell was raised a short distance above the silver ground plane and is bathed on all sides by flowing, fresh, temperature-controlled EAPW.

Data Reduction

A typical response curve is shown in Fig. 3. Since the lower 3-db point of the filters at 0.13 Hz distorts the behavior of the offset at

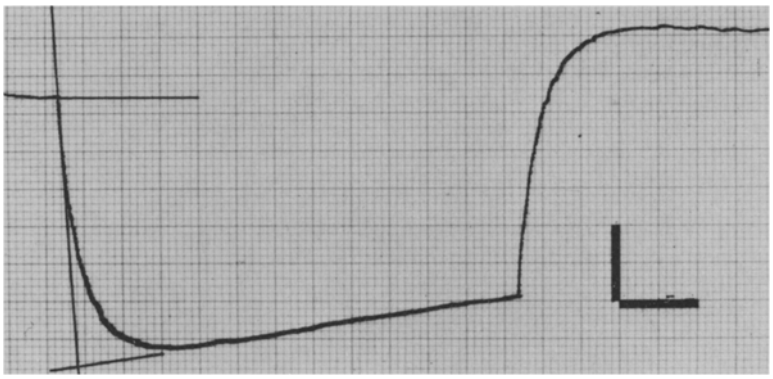

Fig. 3. Typical 20-pulse, intracellular response curve showing the auxiliary lines drawn for data reduction. Pertinent data: internodal cell of *N. flexilis*; resting potential, −70 mV; irradiation frequency, 1.00 MHz; drive voltage amplitude at microstrip, 10.0 V rms; temperature, 25 °C. The vertical bar is 250 μV, the horizontal bar 40 msec; hence the offset height was 900 μV (hyperpolarizing) and the rise time was roughly 8 msec

long times, considerable compensation is required if the true shape of the offset is to be recovered. A simple approximate algorithm was developed as follows. It was assumed (i) that the true signal was a linear combination of a fast rectangular pulse of height ΔV[V] and functional form $\Delta V[1-e^{-t/\tau}]$ where τ[sec] is a time constant and a ramp of slope V'[V/sec] and (ii) that the high pass effect could be represented by a standard, one pole, passive RC filter. Then, neglecting the low pass effects, the system output voltage to the averager will be

$$v_{out}(t)=\mathbf{G}\left[\Delta V\frac{RC}{RC-\tau}(e^{-t/RC}-e^{-t/\tau})+RC\,V'(1-e^{-t/RC})\right] \tag{10}$$

where RC[sec^{-1}] is the time constant of the filter and $\mathbf{G}$[V/V] is the midrange gain of the system. A low frequency 3-db point of 0.13 Hz corresponds to an RC of roughly 1 sec, and the τ to be encountered are very much smaller than this. Thus, for $\tau \ll t \lesssim 250$ msec,

$$v_{out}\doteq\mathbf{G}\left[\Delta V+t\left(V'-\frac{\Delta V}{RC}\right)\right],\quad \tau\ll t\ll RC. \tag{11}$$

And a linear extrapolation back to zero time will yield the height of the distorted pulse. On the other hand, for $t \ll \tau$,

$$v_{out}\doteq\mathbf{G}\Delta V\frac{t}{\tau},\quad 0<t\ll\tau. \tag{12}$$

And a linear extrapolation to the level $\mathbf{G}\,\Delta V$ will yield an estimate of τ.

Therefore the following simple algorithm was adopted for analysis of the offsets:

(i) Draw a baseline through the trace for negative time.

(ii) Draw a mean slope through the initial few milliseconds of the offset. The intersection of this slope with the baseline determines zero time. Its intersection with the level $\mathbf{G}\,\Delta V$ (yet to be found) determines τ.

(iii) Draw a mean slope through a linear portion of the offset in the 50–250 msec range. The height of this line at zero time determines $\mathbf{G}\,\Delta V$.

Experience with many hundreds of records has shown this technique to fit satisfactorily almost all traces.

Some sort of normalization of the raw ΔV data proved necessary because (i) the biological variability among cells made direct intercomparison difficult and (ii) the voltage division of the applied field by the membrane capacitance made it infeasible to use the same microstrip drive voltage at all frequencies and generally 4 V rms was employed below 1 MHz and 10 V rms was employed at and above 1 MHz. The following normalization procedure was adopted:

(i) It was assumed that, if V_{rms}[V] is the drive voltage and f[Hz] the drive frequency, then

$$\Delta V=-K\frac{V_{rms}^{\alpha}}{f^{\beta}} \tag{13}$$

$V_{rms}\leqq 10$ at any frequency or $f\leqq 10^6$ at any voltage where α and β are positive constants; this seemed to be in accord with experiment. Then α and β were determined for the cell by plotting the raw data on full-logarithmic paper. If ΔV *vs.* V_{rms} data were not available, α was set equal to 2. If ΔV *vs.* f data were not available, β was set equal to 2.

(ii) The reference offset $\tilde{V}$[V] was taken to be that at 10 V rms microstrip drive voltage and 1 MHz. If a measured value of $\tilde{V}$ was available, it was used; if not, one was inferred using Eq. (13) on those data closest to the desired point.

(iii) Curves of ΔV *vs.* f at fixed voltage were normalized by (a) plotting them on full-logarithmic paper, (b) extrapolating to a value V_f[V] at 1 MHz by using Eq. (13), (c) finding a constant K_f such that $V_f K_f=\tilde{V}$, and (d) computing the normalized values from

$$\{\Delta V\}_N=\frac{\Delta V K_f}{\tilde{V}}. \tag{14}$$

(iv) Curves of ΔV *vs.* V_{rms} at fixed frequency were normalized by (a) plotting on full-logarithmic paper, (b) extrapolating to a value V_V at 10 V/rms using Eq. (13), (c) finding a constant K_V such that $V_V K_V=\tilde{V}$, and (d) computing the normalized values from

$$\{\Delta V\}_N=\frac{\Delta V K_V}{\tilde{V}}. \tag{15}$$

In the figures to follow, the data points for each group of cells are accompanied by the notation $\tilde{V}=X\pm Y(Z)$ where X is the mean value of $\tilde{V}$, Y is the standard error of the mean, and Z is the number of cells in the sample. Throughout this paper, the statistical characteristics of other quantities will be similarly specified.

Results

Artifacts and Interference

In examining offsets of the magnitude of many of those reported here, an inescapable question is whether they are of true biological origin or are

Fig. 4. A typical artifact check. No cell was present in the channel, but the signal pipette was positioned only 2 mm from the center conductor to increase pickup. $V_{rms} = 10$ V, $f = 1$ Mz, and pulse length = 250 msec. The horizontal bar is 40 msec, the vertical 10 μV. The vertical calibration is for *signal*; to find the approximate conversion from averaged peak-peak displayed noise measured in signal units to rms Gaussian noise referred to the input, it is necessary (i) to divide by 6.6 to convert to rms and (ii) to multiply by $\sqrt{N}$ to compensate for the cancellation of the random noise as compared to the signal. Thus, since 60 Hz cancellation was employed and $N = 40$, the trace corresponds to an input noise of roughly 5 μV rms. Averaging has reduced this sufficiently to make visible in the display step offsets of roughly 1 μV

artifacts of the exposure system or both. And, in fact, two artifacts were discovered which mimic the true biological response.

First, both the input amplifier and the ac amplifier (*cf.* Fig. 1*B*) had slight frequency-dependent nonlinearities which caused them to rectify RF weakly. For example: at 250 kHz, the input amplifier produced an offset which was proportional to the square of the input RF and was roughly 93 μV at an input of 10 mV rms; at 50 or 100 mV rms input, it rose as the second power of the frequency to a rough plateau beginning around 500 kHz. This problem was resolved by adding the passive input filter to attenuate drastically the RF picked up by the pipettes.

Second, the silver electrodes of the microstrip (*cf.* Fig. 2) could themselves rectify weakly if they became corroded. They were, therefore, kept scrupulously clean.

As a precaution, at the start of irradiation each day, a run was made to test for the presence of artifactual offsets. A trace from a typical experiment is reproduced in Fig. 4. Obviously, no artifact is visible at the 1 μV level as there is no net offset beginning about 40 msec from the left margin of the trace. The figure also reveals that the system noise is roughly 5 μV rms referred to input; for comparison, the thermal noise expected from a signal source of 1 MΩ output impedance is the classical Johnson-Nyquist value (*cf.* King, 1966) of roughly 5 μV rms.

Residual 60 Hz pickup was largely magnetic in origin and therefore was not eliminated by use of the radio-frequency shielded room and the Faraday cage made from aluminum screening. It correlated strongly with electrical usage elsewhere in the building, being large during the normal working day and negligible most evenings and weekends. It was cancelled where necessary by the following protocol:

(i) All irradiation bursts were synchronized with the 60 Hz line power, and 60-Hz interference was therefore seen as a "frozen" waveform of 16 2/3 msec duration on the signal averager display rather than as increased tangential noise.

(ii) If, at the conclusion of a 20-pulse summation, the signal averager display showed unacceptable 60 Hz, the leads to the averager's differential input were reversed, V_{rms} set to zero, and 20 more pulses summed. This left the offset unchanged, removed the 60 Hz, and increased the background noise by a factor of $\sqrt{2}$.

Cell Electrical Parameters

The membrane conductivities and capacivities of the cells studied were occasionally measured and were found to be of the same magnitudes as those quoted by other investigators for characean cells (e.g. Bernhardt & Pauly, 1974; Coster & Smith, 1977; Kishimoto, 1972). The values observed at 25 °C were: for *C. braunii* ranges (0.5, 1.3) S/m^2 and (4.5, 7.1) mF/m^2 with means of very roughly $0.8 \pm 0.1\,(7)$ S/m^2 and $5.6 \pm 0.4\,(7)$ mF/m^2; for *N. flexilis* ranges (0.7, 1.4) S/m^2 and (4.9, 8.0) mF/m^2 with means of very roughly $1.0 \pm 0.1\,(7)$ S/m^2 and $6.0 \pm 0.3\,(7)$ mF/m^2. These values imply membrane space constants in the 10 mm range and membrane time constants in the 10 msec range for both species.

Extracellular Response

Suppose that, as is the case here, only a portion of a long cylindrical cell is subjected to RF irradiation. Then it follows that only a portion of the cell could have a rectified current injected by the applied field, and any current so injected should leak out electrotonically over the remainder of the cell. Thus, a

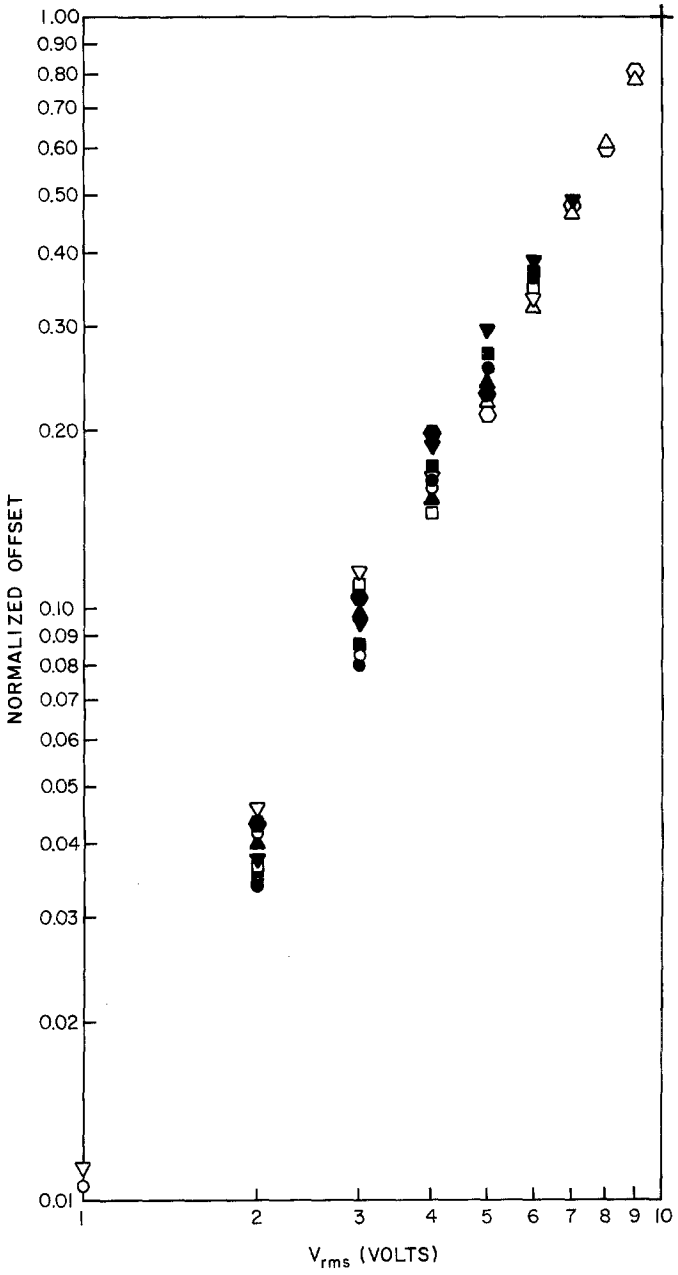

Fig. 5. Normalized extracullarly observed offsed offset $\{\Delta V\}_n$ *vs.* microstrip voltage V_{rms}. The hollow symbols are for five cells of *Chara braunii*; these cells had a mean $\tilde{V}$ of -0.038 ± 0.008 (5) mV. The solid symbols are for five cells of *Nitella flexilis*; these cells had a mean $\tilde{V}$ of -0.028 ± 0.006(5) mV. The cross (+) denotes the normalization point

complete circuit for a line of current would be a closed loop which crosses the plasma membrane in the irradiation region, runs down the cell, leaves at some point in the irradiation-free zone, and swings back extracellularly to its starting point. And because the extracellular medium is of low conductivity this current flow should produce detectable voltage offsets in the extracellular medium; moreover, the magnitude of these offsets should vary with the placement of the signal and reference pipettes. Such offsets were detected with ease.

Table 1. Characteristics of the extracellular response

	Chara braunii	*Nitella flexilis*
$\tilde{V}$ (mV)		
Range	(−0.016, −0.085)	(−0.012, −0.076)
Mean	-0.049 ± 0.006 (11)	-0.044 ± 0.005 (13)
α		
Range	(1.9, 2.1)	(1.8, 2.1)
Mean	2.00 ± 0.04 (6)	1.94 ± 0.05 (5)
β		
Range	(1.8, 2.3)	(1.5, 1.6)
Mean	1.95 ± 0.07 (6)	1.54 ± 0.02 (9)
τ (msec)[a]		
Range	(8, 32)	(16, 44)
Mean	17.6 ± 2.1 (11)	22.4 ± 2.3 (13)

[a] These means are for the rise times measured directly at the normalizing point $f = 1$ MHz and $V_{rms} = 10$ V.

Figure 5 illustrates the variation with voltage of such an offset. The α-exponent of these pooled data is 2. Further characteristics of the response are given in Table 1.

Figure 6 illustrates the variation with frequency of such an offset. The β-exponents of these pooled data are roughly 2 for *Chara* and $\frac{3}{2}$ for *Nitella*. Further characteristics of the response are given in Table 1.

The time constant of the offset displayed no discerned variation with either voltage or frequency.

Intracellular Response of Nonelectrogenic Cells

In the experience of this laboratory (e.g., Pickard, 1973, or Roa & Pickard, 1976), characean resting potentials are either less negative than −90 mV or more negative than −125 mV; stable resting potentials in the band (−90, −125) are almost never encountered. With cells bathed in EAPW, the region above −90 mV could conceivably be achieved by passive diffusion mechanisms (*cf.* Pickard, 1973), and cells in that region will be designated nonelectrogenic; on the other hand, the region below −125 mV could be achieved only if the resting potential contained a component due to active transport, and cells in that region will be designated electrogenic. The data of this subsection will concern nonelectrogenic cells exclusively, the data on electrogenic cells being reserved for a later subsection.

Figure 7 illustrates the variation with voltage of the intracellularly measured offset of nonelectrogenic cells. As expected, the α-exponent of the pooled data is

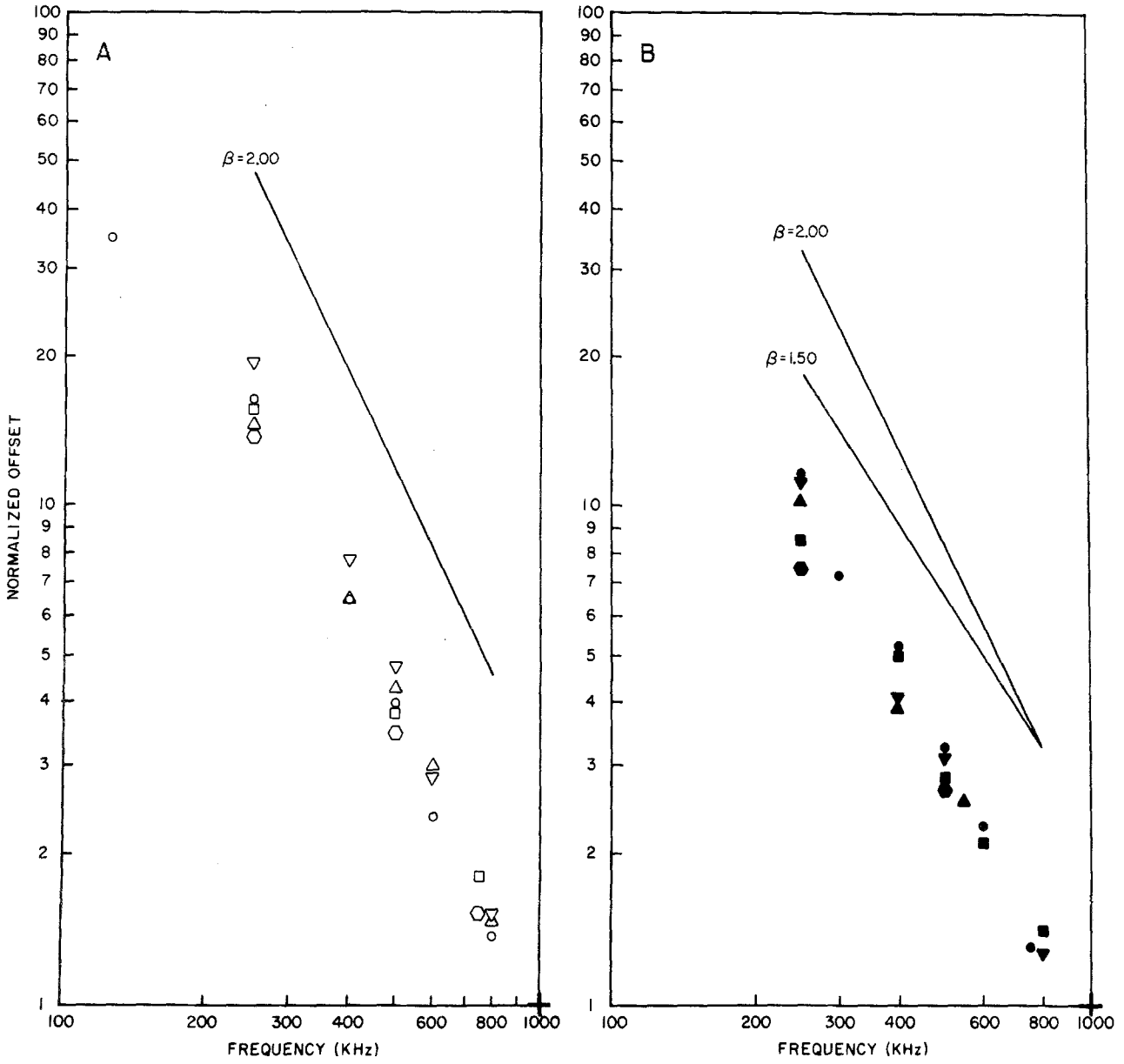

Fig. 6. Normalized extracellularly observed offset $\{\Delta V\}_n$ *vs.* irradiation frequency *f*. (*A*): Data for five cells of *Chara braunii;* the mean $\bar{V}$ of these five cells was $-0.063 \pm 0.008\,(5)$ mV. (*B*): Data for five cells of *Nitella flexilis;* the mean $\bar{V}$ of these five cells was $-0.049 \pm 0.009\,(5)$ mV. The cross (+) denotes the normalization point

roughly 2. Further characteristics of the response are given in Table 2.

Figure 8 illustrates the variation with frequency of the offset. Note the f^{-2} variation below 4 MHz, the seemingly faster decline from 4 to 10 MHz, the apparent tendency to "bounce around" between 4 and 10 MHz, and the lack of detectable offset above 15 MHz; this is not inconsistent with the transit time-limited rectification mechanism proposed above. Further characteristics of the response are given in Table 2.

Putatively Thermal Effects

Above 15 or 20 MHz, no offset is measurable. But this does not, as can be seen from an examination of Fig. 9, mean that there is not a visible effect. At the low frequency shown in Fig. 9*A*, one sees the usual offset (ostensibly from rectification) which was illustrated in Fig. 3; the positive slope at large times is due to the high pass characteristics of the filters. As *f* is increased to the intermediate frequency, the positive slope gradually decreases and becomes zero.

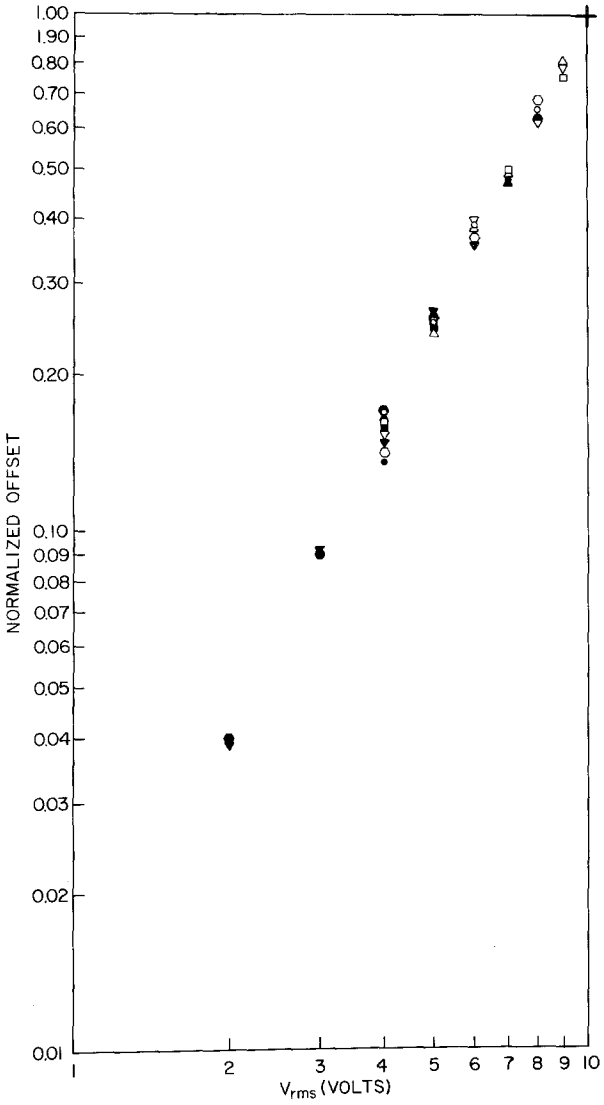

Fig. 7. Normalized intracellularly observed offset $\{\Delta V\}_n$ *Vs.* microstrip voltage V_{rms}. The hollow symbols are for five cells of *Chara braunii*; these cells had a mean $\tilde{V}$ of $-0.49 \pm 0.03(5)$ mV and a mean resting potential of $-80 \pm 3(5)$ mV. The solid symbols are for five cells of *Nitella flexilis*; these cells had a mean $\tilde{V}$ of $-0.72 \pm 0.16(5)$ mV and a mean resting potential of $-73 \pm 6(5)$ mV. The cross (+) denotes the normalization point

Table 2. Characteristics of the intracellular response

	Chara braunii	*Nitella flexilis*
$\tilde{V}$ (mV)		
Range	(−0.2, −1.2)	(−0.2, −1.3)
Mean	$-0.53 \pm 0.07(15)$	$-0.67 \pm 0.06(24)$
α		
Range	(1.8, 2.1)	(1.8, 2.1)
Mean	$1.99 \pm 0.03(14)$	$1.95 \pm 0.03(11)$
β (0.25–1.00 MHz)		
Range	(1.7, 2.3)	(1.7, 2.1)
Mean	$1.83 \pm 0.04(15)$	$1.81 \pm 0.02(14)$
τ (msec)[a]		
Range	(8, 24)	(8, 42)
Mean	$11.9 \pm 1.1(15)$	$21.9 \pm 1.8(24)$
Resting potential (mV)		
Range	(−60, −90)	(−32, −89)
Mean	$-83 \pm 3(15)$	$-58 \pm 4(24)$

[a] These means are for the rise times measured directly at the normalizing point $f = 1$ MHz and $V_{rms} = 10$ V.

And as f is increased further to the high frequency, ΔV goes to zero and the slope assumes a negative value. This behavior is what would, from Eq. (11), be expected as $\Delta V \to 0^-$ if $V' < 0$ and if the unfiltered response is indeed a linear combination of a hyperpolarizing step and a hyperpolarizing ramp. That the ramp seen in the high frequency trace of Fig. 9 can be labeled "putatively thermal" is demonstrated as follows. First, the principal electromagnetic loss mechanism at and below 50 MHz should be purely ohmic and result in frequency-independent heating of the bathing medium because the Debye-Falkenhagen effect is weak at the ionic strengths (< 10 mM) used. Therefore the thermal effect of the irradiation pulse, which *must* exist at some level of irradiation intensity and equipment sensitivity, should also be frequency independent. The slopes observed in several cells, normalized to that at 20 MHz, are shown in Fig. 10; no frequency dependence is apparent. Second, if the slopes are due to a thermal offset of the resting potential and if this offset achieves an asymptotic level in a time period comparable to the inferred thermal time constants of the system, then the response of the cell to pulses of high frequency irradiation several seconds long should show (a) the negative ramp followed after perhaps 800 msec by (b) a rollover to a positive ramp induced by the high pass filtering. The measured, stretched-pulse response was found to be precisely that. Third, if indeed the slope is thermal it should vary linearly with the electrical power delivered or as V_{rms}^2. Figure 11 demonstrates that this is in fact the case.

Response of the System to Miscellaneous Challenges

In this subsection we report the results of several additional tests designed either to substantiate our claim that the offset is biological in origin and not artifactual or to explore in a preliminary fashion further properties of the offset.

It could perhaps be argued that the observed offset is due to rectification of the RF by the detector amplifiers and that the apparent absence of the effect in the absence of a cell reflects some sort of cell-mediated coupling between microstrip and micropipette. This remote possibility was removed by bypassing the dual passive input filter so that all

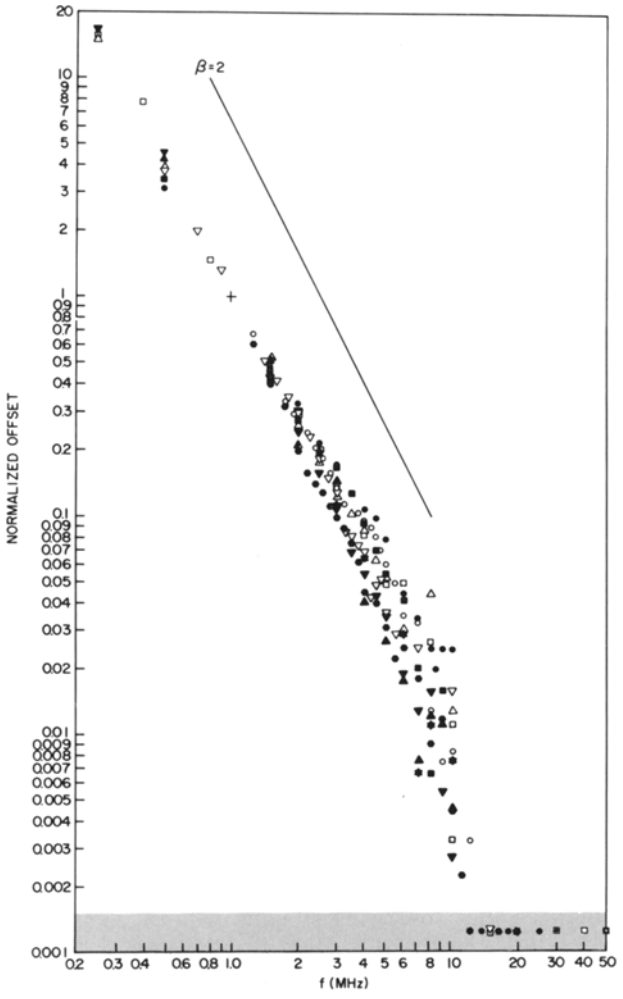

Fig. 8. Normalized intracellularly observed offset $\{\Delta V\}_n$ *vs.* irradiation frequency f. The hollow symbols are for four cells of *Chara braunii*; these cells had a mean $\tilde{V}$ of $-0.68 \pm 0.23(4)$ mV and a mean resting potential of $-76 \pm 8(4)$ mV. The solid symbols are for six cells of *Nitella flexilis*; these cells had a mean $\tilde{V}$ of $-0.55 \pm 0.11(6)$ mV and a mean resting potential of $-45 \pm 4(6)$ mV. The cross (+) denotes the normalization point. The points in the shaded band are ones for which the offset was not distinguishably different from zero

the picked-up RF entered the amplifiers and observing that, at the levels tested, the measured ΔV was unchanged.

In a series of nine cells, the connection between the extracellular response and the intracellular response was investigated by clipping the end off the cell while extracellular recording was in progress. As might have been expected, elimination of the voltage drop across the cell membrane immediately raised the offset toward, but by no means to, typical intracellular levels. Following this, the offset decayed to zero over the space of a few minutes, presumably signalling membrane death and disorganization.

When the bathing solution was modified to contain 100 μM of 3,4-diaminopyridine, no change was observed in the offset of 4 *Nitella* cells, $\tilde{V}$ being $-0.58 \pm 0.23(4)$ mV in normal EAPW and $-0.56 \pm 0.15(4)$ mV in DAP-EAPW. Since DAP is known to be a potent blocker of passive potassium flux in squid axon (Kirsch & Narahashi, 1978), bullfrog auditory hair cell (Corey & Hudspeth, 1979), and barnacle muscle (Nelson & Blaustein, 1980), we suggest that either (i) the significant current of offset is not carried through potassium channels and/or (ii) that the characean potassium channel is pharmacologically different from the animal channels studied to date.

When the bathing solution was modified to contain 40 μM diethylstilbestrol, no change was observed in the offset unless the resting potential was sensibly abolished (putative cell death); complete collapse of the resting potential, which often occurred at the end of an experiment with 40 μM DES, was invariably accompanied by abolition of the offset. This concentration of DES was believed by Keifer and Spanswick (1978) to inhibit strongly electrogenic ion pumping in *Chara corallina*. Since the cells studied in this paper had, with rare exceptions, resting potentials derivable from passive fluxes alone, this lack of effect buttresses the suspicion that the offset is due to interference with passive charge transfer processes.

The measured conductivity of characean membrane is commonly found to be monotone, increasing with temperature (e.g., Pickard, 1973). Although this conductivity may be largely a reflection of active processes (*cf.* Keifer & Spanswick, 1978; Fujii,

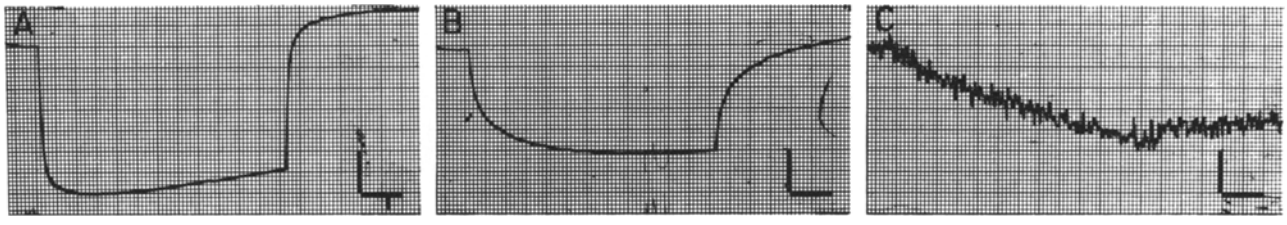

Fig. 9. Displayed intracellular offsets at $V_{rms} = 10$ V and three different frequencies for a cell of *Chara braunii*. The resting potential was −82 mV. The horizontal bar is 40 msec in all cases. (*A*): 1 MHz with the vertical bar equal to 250 μV; (*B*): 2 MHz with the vertical bar equal to 125 μV; (*C*): 20 MHz with the vertical bar equal to 10 μV

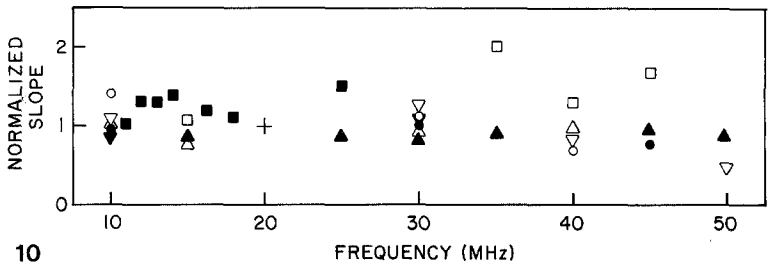

Fig. 10. Normalized slope of intracellular response versus frequency for characean cells irradiated at a microstrip voltage of $V_{rms}=10$ V. The hollow symbols are for *Chara braunii;* these cells had a mean slope at 20 MHz of $-0.065\pm0.009(4)$ mV/sec and a mean resting potential of $-78\pm6(4)$ mV. The solid symbols are for *Nitella flexilis;* these cells had a mean slope at 20 MHz of $-0.068\pm0.007(4)$ mV/sec and a mean resting potential of $-73\pm11(4)$ mV. The cross (+) denotes the normalization point

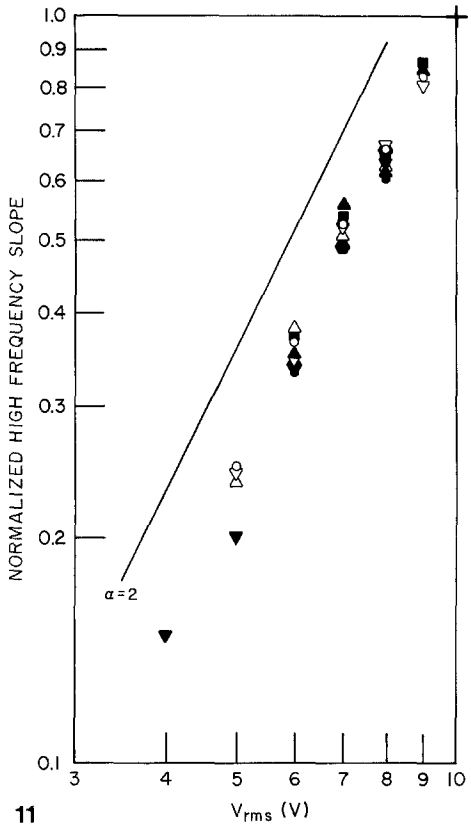

Fig. 11. Normalized slope of intracellular response *vs.* V_{rms} for *Chara* cells (hollow symbols) irradiated at 10 MHz, for *Nitella* cells (most solid symbols) irradiated at 10 MHz, and for a single *Nitella* cell (▲) irradiated at 30 MHz. The solid line is of exponent two, and the cross (+) denotes the normalization point. The mean slopes at $V_{rms}=10$ were $-0.061\pm0.007(3)$ mV/sec for the *Chara* cells and $-0.051\pm0.002(5)$ mV/sec for the *Nitella* cells

Shimmen & Tazawa, 1979), it is reasonable to assume that increasing conductivity should correlate with increasing offset. And indeed, the intracellular effect was found to be monotone increasing in temperature from 10 to 35 °C, being at 10 °C perhaps one-half as large as that at the standard 25 °C and at 35 °C perhaps 50% larger than that at 25 °C. However, the shift in membrane conductivity greatly magnifies these effects extracellularly.

As with virtually all of the characean cells studied in this laboratory over the past decade, the cells in this study were found to have resting potentials which were either more positive than −90 mV or more negative than −125 mV. The former level could conceivably be explained by passive diffusion and cells in that category were therefore called "nonelectrogenic"; the latter level, for cells in EAPW, had to involve an electrogenic contribution and cells in that category were therefore called "electrogenic." The cells reported on thus far were all nonelectrogenic. Occasionally a *Chara* cell would be encountered which was nonelectrogenic upon impalement but which, after some tens of minutes, flipped suddenly into an electrogenic state. When this happened, the offset flipped sign and dropped abruptly in magnitude. For the nonelectrogenic *Chara* states studied $\tilde{V}=-0.53\pm0.07(15)$ mV; while for the electrogenic ones studied $\tilde{V}=+0.040\pm0.010(5)$ mV. Clearly, the offset-producing conduction mechanisms of these two states differ greatly; but this is not surprising since the states themselves are known to differ in various other essential aspects (*cf.* Walker, 1980).

Discussion

Are the Observed Offsets Due to Rectification?

The principal predictions of the theory of the proposed rectification mechanism are: (i) The offsets should vary as V_{rms}^2. (ii) As a result of membrane capacitance effects, the offsets should vary as f^{-2} below 1 MHz. (iii) The rise times of the offsets should approximate the rise times classically determined for the cells. (iv) The offset should display transit time effects at sufficiently high frequencies.

The V_{rms}^2 variation was universally observed (cf. Figs. 5 and 7 and Tables 1 and 2).

The f^{-2} variation at low frequencies was observed in the extracellular response of *Chara braunii* (*cf.* Fig. 6*A* and Table 1), but (a) was only roughly fulfilled in the intracellular response (*cf.* Fig. 8 and Table 2) and (b) was not seen in the extracellular response of *Nitella flexilis* (*cf.* Fig. 6*B* and Table 1) where the variation was as $f^{-3/2}$. Since the $f^{-3/2}$ response of *Nitella* was seen in numerous cells over several months during which *Chara* cells gave the expected quadratic variation, it is probably real. We

have no firm explanation for this anomaly, especially since the intra- and extracellularly observed values of β were different. However, it should be noted that a nonquadratic response would be expected if either the tonoplast and/or the plasmalemma capacitances varied with frequency, and there is evidence from squid (Takashima, 1979) that the audio frequency capacitance of plasmalemma can fall off with increasing frequency. Moreover, the different exponents observed could conceivably occur if (a) the extracellular pipette reflected mainly cytoplasmic offset and if (b) this behaved differently from the vacuolar offset sensed by the intracellular pipette.

The classical rise time of a membrane is approximately 2.2 C/G or, for the cells used here, very roughly 10–20 msec for both *Chara* and *Nitella*. This overlaps the values reported in Tables 1 and 2.

Effects, ostensibly of transit time origin, do indeed occur in the 10-MHz range (*cf.* Fig. 8). They will be discussed in greater detail later.

We conclude that the experimental observations are consistent with the proposed rectification mechanism for *Chara* and are largely consistent for *Nitella*. In the absence of any known contender mechanisms, we recommend that RF rectification be adopted as a working hypothesis for the offset.

Has the Charge Carrier Transit Time Been Determined?

In considering transit time effects on the vacuolar resting potential of a giant algal cell, it must be borne in mind that the charge is being carried by unknown conduction mechanisms and by a variety of anions and cations (*cf.* Hope & Walker, 1975); further, it must penetrate a cell wall which may have ion exchange properties and two membranes (plasmalemma and tonoplast). Thus transit time will presumably give rise to a far more complex phenomenon than would be generated by electron flow in a vacuum tube or than is described by the highly idealized theory of Appendix II. What would be expected (in common with other transit time phenomena) is that, as $2\pi f\hat{T}$ passes through the range $(1, \pi)$, the basic phenomenon under consideration should drop rapidly to a low level. In the offset data presented here it would be expected that, over little more than an octave of frequency, the offset would drop from an f^{-2} curve to zero and possibly show some comb structure in the process. This is precisely what happens in Fig. 8 where the low frequency curve extrapolates to indistinguishably low levels at roughly 40 MHz but where the actual curve reaches such levels roughly at a frequency of $\hat{f} \doteq 10$ MHz. This value lies within the range predicted by Pickard and Rosenbaum (1978) from *à priori* considerations. If the approximation $2\pi\hat{f}\hat{T} = \pi$ is made, a composite transit time of roughly 50 nsec is obtained; this is somewhat longer than the lower limit of 5 nsec estimated on *à priori* grounds by Pickard and Rosenbaum (1978). For a membrane 8 nm thick with an 80-mV resting potential, this corresponds roughly to an ionic velocity of 0.16 m/sec and an ionic mobility of $1.6 \times 10^{-8} \frac{m^2}{V \cdot sec}$, which is roughly one-fifth that expected for K^+ in free solution[2].

In the absence of a competing explanation for the sudden drop, it is suggested that a transit time cutoff be accepted as a working hypothesis for this phenomenon.

Does the Technique Employed Separate Thermal and Athermal Effects?

In the introduction a two-part test for athermal effects was outlined; it can be applied here as follows. First, classical RF heating should be largely frequency independent in the 0.1–50 MHz range and should be characterized by a time constant in the 1 sec range; the observed offset had a pronounced frequency dependence and a rise time in the 15 msec range. Second, the offset is in accordance with the predictions of an athermal theory. Therefore the offset is athermal.

On the other hand, the small hyperpolarizing ramp seen at higher frequencies behaves in accordance with the predictions of a classical thermal theory and must, therefore, be presumed thermal.

It was the assertion of Pickard and Rosenbaum (1978), who first proposed this pulsed RF experiment, that the key to the dissection of athermal from thermal lay in the time constants of the responses, the athermal being much faster and therefore yielding at small times a step superposed upon a slower thermal ramp. As it turned out, size alone often sufficed for the separation; and, at most frequencies, the thermal was simply swamped. Nevertheless, the time constants of the response did provide confirmatory evidence for the natures of the offset and the ramp. And the step *vs.* ramp concept should provide a sensitive detection and discrimination technique for as yet undiscovered membrane effects in the realm beyond 50 MHz.

---

[2] For comparison purposes, ionic mobilities are readily obtained from the extensively tabulated values of equivalent ionic conductivities. The conversion formula for univalent ions is

$$\text{mobility} = \frac{(\text{equivalent conductivity})}{10000\,F}$$

where $F[=9.64\ldots \times 10^4$ C/mol] is the Faraday.

What Does the Offset Reveal about the Conduction Mechanisms of Characean Membrane?

In as much as the RF rectification offset is a phenomenon which is qualitatively and quantitatively different from anything previously used to study membrane electrophysiology, it seems reasonable to suppose that it should contain information not readily available from other techniques. For example, $\tilde{V}$ should (*cf.* Pickard & Rosenbaum, 1978) contain information on the nonlinearities of the conduction mechanism; and $\hat{T}$ should reveal something of the nature of the channel. On the other hand, *detailed* investigations of charge transfer mechanisms in the characeae are quite possibly not practicable by the RF rectification technique because of the number of ions and membranes involved. In a preparation such as the squid axon, where the several charge transfer mechanisms can be selectively poisoned, offset measurements could prove more readily interpretable and therefore far more valuable. Nevertheless, the measurements gathered can be interpreted so as to suggest some intriguing possibilities.

First, a plot of resting potential *vs.* $\tilde{V}$ for the twenty-nine cells of Table 2, revealed no readily discernible relationship between these two variables; these cells all possessed resting potentials more positive than -90 mV. However, many *Chara* cells, after spending considerable time at resting potentials between -60 and -90 mV, suddenly flipped to resting potentials more negative than -125 mV; this behavior is entirely normal for the strain employed and has long been interpreted (e.g., Pickard, 1973; Roa & Pickard, 1976) as a consequence of the development of a powerful electrogenic component to the resting potential. Whenever this transition occurred, $\tilde{V}$ immediately shifted from its normal level near half a millivolt negative to a new level near 0.040 millivolt positive. A shift so abrupt is most readily interpreted as a profound qualitative change in the putatively passive (*see* below) conduction mechanisms responsible for the offset, a change that is suggestively correlated with the onset of readily discernible electrogenic ion pumping. And in fact, a cell in the nonelectrogenic state is commonly believed (*cf.* Walker, 1980) to behave somewhat like a potassium electrode, whereas a cell in the electrogenic state is thought to be relatively indifferent to external potassium but rather more sensitive to external pH. Therefore these data would be consistent with the hypothesis that the electrogenic cell not only pumps hydrogen (or hydroxyl) but also develops a dominant passive conductance for it, as well.

Second, the notion of transit time through membranes has been introduced previously (e.g., Pickard & Rosenbaum, 1978; Hardt, 1979). But, as far as is known, this paper is the first in which a direct experimental determination of it has been attempted[3]. The effective mobilities calculated from the inferred transit times are of the order of magnitude expected if the transiting ion moves several-fold more slowly in the membrane than in free solution; and a slowdown of this magnitude seems not unreasonable. The techniques introduced by Hille (1970) for calculating interarrival times of ions at channel mouths yield predictions in the 10 nsec range. This is somewhat less than the inferred transit time and suggests that the principle variety of ion channel in the Characeae is filled much of the time.

Should the Rectification Offset be Deemed a Biological Hazard?

Although the existence of athermal electromagnetic effects is of great intrinsic interest, the efforts of researchers over the last decade have been driven primarily by a need to know whether the present proliferation of radio frequency and microwave sources constitutes a hazard to life and health. And since human exposure to these sources is almost always at low power levels, the question really becomes one of whether there are *potent* athermal effects which were not considered in setting the present thermally oriented exposure standards (*cf.* Steneck, Cook, Vander & Kane, 1980). The RF rectification offset appears to be an athermal effect. But it is to be doubted that it is of sufficient magnitude over the frequency range studied to be termed "potent." To be sure, half millivolt offsets of the resting potentials of cells could be significant. But where are the 10^4 V/m (inside the body) driving fields to come from? A driving field of strength E_{rms} in air will (*cf.* Appendix I) produce a macroscopic internal field of only $E_i = E_{\text{rms}} \dfrac{2\omega\varepsilon_0}{\sigma_i}$ in a flesh cylinder of conductivity σ_i; and if $\sigma_i \approx 1$ S/m, this is an attenuation of at least 1000-fold at frequencies below the transit time cutoff. Moreover, the E_i will give rise to an energy deposition of (*cf.* King, 1963) $\sigma_i E_i^2$ per unit volume; and, as the body itself is presumed to generate less than 100 W (*cf.* Pound, 1980), a continuous E_i of even 10^2 V/m should be excruciatingly obvious and should have been considered as a thermal hazard. Only if there are available occasionally pulsed sources capable of generating E_{rms} in excess of 10^5

[3] This measure of transit time must be distinguished from occasional measures of charge redistribution time (*cf.* Cole, 1968) which, as a result of membrane capacitance effects, is actually a different quantity.

V/m outside their supposedly shielded enclosures, should this effect pose even the possibility of an athermal threat. Pulsed sources of such power are rare to nonexistent over the frequency band studied here.

We wish to thank the National Science Foundation for support under grant ENG7808412 and Professor Fred J. Rosenbaum for much valuable advice and encouragement along the way.

Appendix I

The boundary value problem of the cylindrical cell in a uniform external field translates into a problem with Laplace's equation if the cell radius is very much less than the wavelength of the applied field. Let $\Phi[V]$ be the phasor electric scalar potential. Then, if the cell is placed at the origin of a cylindrical (r, θ, z) coordinate system with its axis coincident with the z-axis,

$$\nabla^2 \Phi_e = 0, \quad r > a \tag{A.I.1}$$

$$\nabla^2 \Phi_i = 0, \quad r < a. \tag{A.I.2}$$

The appropriate boundary conditions are

$$\lim_{r \to \infty} \Phi_e = -\sqrt{2} E_{\text{rms}} r \cos\theta \tag{A.I.3}$$

$$\lim_{r \to 0} \Phi_i = \text{finite} \tag{A.I.4}$$

$$-\frac{\partial \Phi_i}{\partial r}(\sigma_i + j\omega\varepsilon_i) = (\Phi_i - \Phi_e)Y$$

$$= -\frac{\partial \Phi_e}{\partial r}(\sigma_e + j\omega\varepsilon_e), \quad r = a \tag{A.I.5}$$

where Eq. (A.I.5) is the appropriate continuity condition on the electric field vector in the limit of an infinitely thin plasma membrane (*cf.* King, 1963). These equations are readily solved by classical separation of variable techniques to yield

$$\Phi_i = [\sqrt{2} E_{\text{rms}} r \cos\theta] \frac{-2\frac{\zeta_e}{\zeta_i}}{\left[\left(1 + \frac{\zeta_e}{\zeta_i}\right) + \frac{\zeta_e}{aY}\right]} \tag{A.I.6}$$

and

$$\Phi_e = \left[\sqrt{2} E_{\text{rms}} \frac{a^2 \cos\theta}{r}\right] \frac{1 - \frac{\zeta_e}{\zeta_i} - \frac{\zeta_e}{aY}}{\left(1 + \frac{\zeta_e}{\zeta_i}\right) + \frac{\zeta_e}{aY}}$$

$$- [\sqrt{2} E_{\text{rms}} r \cos\theta], \tag{A.I.7}$$

where $\zeta = \sigma + j\omega\varepsilon$. But the transmembrane voltage is just

$$v(\theta, \omega; t) = \mathscr{R}\mathscr{e}\{e^{j\omega t}[\Phi_i - \Phi_e]_{r=a}\} \tag{A.I.8}$$

so that the desired formula is

$$v(\theta, \omega; t) = [a\sqrt{2} E_{\text{rms}} \cos\theta]\, \mathscr{R}\mathscr{e}\left\{\frac{2\frac{\zeta_e}{aY} e^{j\omega t}}{\left(1 + \frac{\zeta_e}{\zeta_i}\right) + \frac{\zeta_e}{aY}}\right\}. \tag{A.I.9}$$

For a typical characean cell (Hope & Walker, 1975) the internal anion concentration is roughly 150 mM implying $\sigma_i \approx 1$, while $G \ll 10$, $C \approx 0.01$, and $a \approx 0.2 \times 10^{-3}$; the cells used in the experiments reported here seemed to be crudely comparable. $\varepsilon_i = \varepsilon_e = \varepsilon_{\text{water}} \doteq 7 \times 10^{-10}$. And for the bathing solutions employed, a crude value for the external conductivity is $\sigma_e \approx 0.1$. Thus, above 0.1 MHz, the membrane admittance is to excellent approximation $Y = j\omega C$ while $|\zeta_e/(aY)| \ll 1$. Moreover, in the 0.1–50 MHz band, $|\zeta_e/\zeta_i| \ll 1$.

Hence Eq. (A.I.9) reduces to

$$v(\theta, \omega; t) \doteq [2\sqrt{2} E_{\text{rms}} \cos\theta]\, \mathscr{R}\mathscr{e}\left\{\frac{\zeta_e}{j\omega C} e^{j\omega t}\right\} \tag{A.I.10}$$

for frequencies between 0.1 and 50 MHz.

Appendix II

In this Appendix the problem of transit time will be treated. First, a definite model for conduction will be proposed and its transit time behavior worked out. Of course, the present state of knowledge on the behavior of ion channels in the Characeae does not warrant this degree of concreteness, but the exercise will serve to illustrate the sorts of considerations involved. Second, a more general heuristic argument will be advanced to show that a roughly similar form of behavior would be expected, independent of the detailed behavior of the channels involved.

Consider an infinite planar membrane lying between $x = 0$ and $x = L$ within which the mean velocity of a certain species charge carrier is specified by the linear characteristic

$$\frac{dx}{dt} = S + \frac{\mu}{L}\sqrt{2} v_o \cos(\omega t + \psi) \tag{A.II.1}$$

where S [m/sec] is the drift velocity of the carrier in the absence of the applied voltage $\sqrt{2} v_o \cos(\omega t + \psi)$, ψ [rad] is a phase parameter, and $\mu\left[\frac{\text{m}^2}{\text{V} \cdot \text{sec}}\right]$ is the carrier mobility: it is assumed that the carrier is moving with the steady field imposed by the resting potential. For the normal case in which S is due to a substantial membrane potential and to diffusion while v_o is quite small compared to the resting potential, the S term of Eq. (A.II.1) will dominate. If then a carrier appears in the membrane at ($x = 0$, $t = 0$) and leaves at ($x = L$, $t = T$), it follows from (A.II.1) that

$$L = ST + \frac{\sqrt{2}\mu v_o}{L\omega}[\sin(\omega T + \psi) - \sin\psi]. \tag{A.II.2}$$

If now the channel remains empty for a waiting time $\hat{W}$ [sec] following the passage of an ion then the current per unit area must vary as $(T + \hat{W})^{-1}$. But, since each cell will possess two sides and since (*cf.* Appendix I) switching sides merely changes the sign of v_o, the total shift in current most obey the rule

$$\Delta I \propto \frac{1}{T_+ + \hat{W}} + \frac{1}{T_- + \hat{W}} - \frac{2}{\hat{T} + \hat{W}} \tag{A.II.3}$$

where $\hat{T} = L/S$ and T_+ and T_- are the solutions of Eq. (A.II.2) with v_o, respectively, positive and negative. A perturbation expansion in v_o of T about $\hat{T}$ in (A.II.2) enables (A.II.3) to be reduced to

$$\Delta I \propto \left[\frac{\mu/(LS)}{1 + \frac{\hat{W}}{\hat{T}}}\right]^2 \frac{v_o^2}{(\omega\hat{T})^2}\left[-\beta_2 + \frac{\beta_1^2}{\hat{T} + \hat{W}}\right] \tag{A.II.4}$$

where it has been assumed that $\omega(T_+ - T_-) \ll 1$ and that $\left|\frac{\mu v_o}{L\omega S}\right| \ll \hat{T}$ and where

$$\beta_1 = \sin\psi - \sin(\omega\hat{T} + \psi) \tag{A.II.5}$$

$$\beta_2 = -\omega[\sin\psi \cos(\omega\hat{T} + \psi) - \tfrac{1}{2}\sin(2\omega\hat{T} + 2\psi)]. \tag{A.II.6}$$

However, ψ is randomly distributed over $(0, 2\pi)$, and therefore the average value of ΔI is

$$[\Delta I]_{\text{av}} = \frac{1}{2\pi}\int_0^{2\pi} \Delta I\, d\psi \propto v_o^2\left[\frac{\sin\omega\hat{T}}{2\omega\hat{T}} - \frac{1}{1 + \frac{\hat{W}}{\hat{T}}}\frac{1 - \cos\omega\hat{T}}{(\omega\hat{T})^2}\right]. \tag{A.II.7}$$

Both of the bracketed terms in Eq. (AII.7) display crudely similar behaviors in that they are largest at $\omega\hat{T}=0$, are relatively unchanged at $\omega\hat{T}=1$, fall off rapidly for larger ω, and oscillate as $\omega\hat{T}$ increases beyond π.

A real membrane will presumably have several different types of charge carrier, each of which behaves with less simplicity than that considered above. And this will greatly complicate the form of $[\Delta I]_{av}$. Therefore, since $\Delta V \propto [\Delta I]_{av}$, it can be presumed only that

$$\Delta V = \alpha_2 v_o^2 F(\omega\hat{T}) \qquad \text{(AII.8)}$$

where $F(\omega\hat{T}) \doteq 1$ for $\omega\hat{T} < 1$, where $F(\omega\hat{T})$ then falls off to zero for $\hat{\omega}\hat{T} \approx \pi$, and where $F(\omega\hat{T})$ may exhibit a complicated (but low amplitude) comb structure for $\omega\hat{T} \gtrsim \pi$, a structure somewhat reminiscent of $\sin\omega\hat{T}/\omega\hat{T}$. This general form of frequency behavior seems characteristic of transit time devices in general (*cf.* Dascălu, 1974). That it should also be characteristic of an arbitrary type of ion channel can be shown heuristically as follows. Consider a cell membrane across which a small alternating voltage $v(\omega t)$ is impressed. If $\omega\hat{T} \ll 1$, a transiting ion will see a sensibly constant field and classical rectifier behavior (*cf.* Pickard & Rosenbaum, 1978) should be observed. As $\omega\hat{T}$ increases, some ions will come to see both signs of the impressed voltage and the net rectification will decrease. This decline will continue until $\omega\hat{T}=2\pi$, at which point the effects of accelerating and retarding impressed voltage will have cancelled out. Beyond $\omega\hat{T}=2\pi$ a new cycle will start; but ions entering with different ψ will of course attenuate it significantly. However, a cell has two sides, and the sign of impressed voltage should be opposite on them. Therefore the leading term of a series expansion for the rectifier current should be quadratic in $v(\omega t)$. Since squaring an alternating voltage is well known to effect a frequency doubling, it would be reasonable to expect the first zero of the rectifier current to be shifted downward toward $\omega\hat{T}=\pi$. That is, Eq. (AII.8) and the form of $F(\omega\hat{T})$ described above are plausible. However, it must be emphasized that an estimate of $\hat{T}$ from measurements of the first minimum of ΔV should be deemed accurate only to within a factor of two or three since it is not immediately obvious whether $\hat{T}$ should be estimated by the standard approximation Eq. (4), or by the $\omega\hat{T}=\pi$ chosen here, or even by $\omega\hat{T}=2\pi$: the processes of charge transfer through the membrane are not well enough understood to permit more precise specification.

References

Barnes, F.S., Hu, C.L.J. 1977. Model for some nonthermal effects of radio and microwave fields on biological membranes. *IEEE Trans. Microwave Theory Tech.* **25**:742–746

Bawin, S.M., Sheppard, A., Adey, W.R. 1978. Possible mechanisms of weak electromagnetic field coupling in brain tissue. *Bioelectrochem. Bioenerg.* **5**:67–76

Bernhardt, J., Pauly, H. 1947. Dielectric measurements of *Nitellopsis obtusa* cells with intracellular electrodes. *Radiat. Environm. Biophys.* **11**:91–109

Cain, C.A. 1980. A theoretical basis for microwave and rf field effects on excitable cellular membranes. *IEEE Trans. Microwave Theory Tech.* **28**:142–147

Carslaw, H.S., Jaeger, J.C. 1959. Conduction of Heat in Solids. Oxford University Press, London

Cole, K.S. 1968. Membranes, Ions, and Impulses. University of California Press, Berkeley

Cooke, H.F. 1971. Microwave transistors: Theory and design. *Proc. IEEE* **59**:1163–1181

Corey, D.P., Hudspeth, A.J. 1979. Ionic basis of the receptor potential in a vertebrate hair cell. *Nature (London)* **281**:675–677

Coster, H.G.L., Smith, J.R. 1977. Low-frequency impedance of *Chara corallina*: Simultaneous measurements of the separate phasmalemma and tonoplast capacitance and conductance. *Aust. J. Plant Physiol.* **4**:667–674

Dascălu, D. 1974. Transit-Time Effects in Unipolar Solid-State Devices. Abacus, Tunbridge Wells

Fujii, S., Shimmen, T., Tazawa, M. 1979. Effect of intracellular pH on the light-induced potential change and electrogenic activity in tonoplast-free cells of *Chara australis*. *Plant Cell Physiol.* **20**:1315–1328

Hardt, S.L. 1979. Pace of diffusion through membranes. *J. Membrane Biol.* **48**:299–323

Hille, B. 1970. Ionic channels in nerve membranes. *Prog. Biophys. Mol. Biol.* **21**:1–32

Hope, A.B., Walker, N.A. 1975. The Physiology of Giant Algal Cells. Cambridge, London

Keifer, D.W., Spanswick, R.M. 1978. Activity of the electrogenic pump in *Chara corallina* as inferred from measurements of the membrane potential, conductance, and potassium permeability. *Plant Physiol.* **62**:653–661

King, R.A. 1966. Electrical Noise. Chapman & Hall, London

King, R.W.P. 1963. Fundamental Electromagnetic Theory. Dover, New York

Kirsch, G.E., Narahashi, T. 1978. 3,4-diaminopyridine. A potent new potassium channel blocker. *Biophys. J.* **22**:507–512

Kishimoto, U. 1972. Characteristics of the excitable *Chara* membrane. *Adv. Biophys.* **3**:199–226

Lindquist, C.S. 1977. Active Network Design. Steward, Long Beach

Mittra, R., Itoh, T. 1974. Analysis of microstrip transmission lines. *Adv. Microwaves* **8**:67–141

Nelson, M.T., Blaustein, M.P. 1980. Properties of sodium pumps in internally perfused barnacle muscle fibers. *J. Gen. Physiol.* **75**:183–206

Offner, F. 1979. Major inversions of state of a stochastic system resulting from small perturbations: Applications to the excitable membrane. *Bull. Am. Phys. Soc.* **24**:320

Pickard, W.F. 1973. Does the resting potential of *Chara braunii* have an electrogenic component? *Can. J. Bot.* **51**:715–724

Pickard, W.F., Rosenbaum, F.J. 1978. Biological effects of microwaves at the membrane level: Two possible athermal electrophysiological mechanisms and a proposed experimental test. *Math. Biosci.* **39**:235–253

Pound, R.V. 1980. Radiant heat for energy conservation. *Science* **208**:494–495

Roa, R.L., Pickard, W.F. 1976. The use of membrane electrical noise in the study of characean electrophysiology. *J. Exp. Bot.* **27**:460–472

Spiegel, R.J., Joines, W.T. 1973. A semiclassical theory for nerve excitation by a low intensity electromagnetic field. *Bull. Math. Biol.* **35**:591–605

Steneck, N.H., Cook, H.J., Vander, A.J., Kane, G.L. 1980. The origins of U.S. safety standards for microwave radiation. *Science* **208**:1230–1237

Stuchly, M.A. 1979. Interaction of radiofrequency and microwave radiation with living systems. *Radiat. Environm. Biophys.* **16**:1–14

Takashima, S. 1979. Admittance change of squid axon during action potentials. Change in capacitive component due to sodium currents. *Biophys. J.* **26**:133–142

Wachtel, H., Seaman, R., Joines, W. 1975. Effects of low-intensity microwaves on isolated neurons. *Ann. N.Y. Acad. Sci.* **247**:46–62

Walker, N.A. 1980. The transport systems of charophyte and chlorophyte giant algae and their integration into modes of behavior. *In:* Plant Membrane Transport: Current Conceptual Issues. R.M. Spanswick, W.J. Lucas, and J. Dainty, editors. p. 287–304. Elsevier, Amsterdam

Received 9 October 1980; revised 20 January 1981